

Full Length Research Paper

Shear behaviour of palm kernel shell reinforced concrete beams without shear Reinforcement: Influence of beam depth and tension steel

A. Acheampong^{1*}, C. K. Kankam² and J. Ayarkwa¹

¹Department of Building Technology, Kwame Nkrumah University of Science and Technology (KNUST), Ghana.

²Department of Civil Engineering, Kwame Nkrumah University of Science and Technology (KNUST), Ghana.

Received 3 December, 2015; Accepted 3 March, 2016

This study investigated the influence of beam depth with varying longitudinal reinforcement without shear reinforcement. Size effect, which is described here in as the decrease in shear strength with the increase in the depth of members, is not evaluated sufficiently enough. To this end, fifteen palm kernel shell (PKS) reinforced concrete beams varying from 150 to 300 mm were tested to investigate their size effects on ultimate shear capacity and failure modes. Test variables were longitudinal reinforcement ratio (ρ_w varying from 1 to 2%) and effective depth of beams (varying from 120 to 265 mm) with average compressive strength (f_{cu}) = 30.3 MPa and shear span to effective depth (a_v/d) = 2.5. For the range of variables tested, the test results were compared with the strengths predicted by the ACI 318-08 and BS 8110 with and without reduction factors. All tested beams failed in shear failure modes and were influenced by the beam depth and amount of longitudinal reinforcement. The PKS beams were found to develop sufficient strength after diagonal cracking to continuously transfer loads until failure.

Key words: Palm kernel shell concrete, size effects, longitudinal reinforcement, shear strength, ACI 318-08, BS8110.

INTRODUCTION

The increasing demand for concrete products in the construction industry is inevitably challenging engineers to maintain ecological balance with alternative materials. Successfully, the use of both artificial and natural lightweight aggregates for concrete production mark a very significant breakthrough. This is because the use of lightweight aggregate concrete in construction presents many advantages over the normal-weight concrete; notable among them being the increased strength/weight

ratio, improved thermal and sound insulation, and fire resistance properties; which is attributed to the high porosity of the lightweight aggregates. In recent times, the utilization of solid wastes generated from agro-based products such as Palm kernel shells is very essential for the restoration of ecological balance (Mannan and Ganapathy, 2003). It is one of the basic strategies to reduce solid agricultural waste problems in palm oil producing countries (Mannan and Ganapathy, 2003; Loehr, 1984).

*Corresponding author. E-mail: achielex@yahoo.com.

Palm kernel shells (PKS) are obtained from cracking the palm fruits during palm kernel processing. PKS have stony and hard endocarps that protects the palm kernel; the size and thickness of which depend on the species. Okpala (1990); Basri et al. (1999) and Mannan and Ganapathy (2002) have shown that the use of PKS as aggregates can produce structural concrete of compressive strength in excess of 20 N/mm^2 at 28 days with a density in the range of 1800 to 1900 kg/m^3 . The structural behaviour in relation to flexure and bonding has been reported in addition to the mechanical properties of PKS concrete (Teo et al., 2006; Alengaram et al., 2010). Teo et al. (2006) reported that ultimate moments predicted using BS 8110 provides a conservative estimate for PKS concrete beams up to a reinforcement ratio of 3.14%. That notwithstanding, deflections and crack widths at service loads were all reported to be within the maximum allowable values stipulated by BS 8110. Shear resistance of reinforced concrete beams have been a subject of concern for structural designers and researchers for over 50 years now. However, the shear failure modes, the resisting mechanisms at cracked stages, and the role of various parameters are still under discussion and are inconclusive among various researchers. The results of experimental studies reveal that shear failure of a reinforced concrete beam is very complex; involving numerous parameters. Shear span to depth ratio (a/d), tension steel ratio (ρ), compressive strength of concrete (f_c), size of coarse aggregate, density of concrete, size of beams, tensile strength of concrete, support conditions, clear span to depth ratio (L/d), grade of tension reinforcement and end anchorage of tension reinforcement (Ghaffar et al., 2010; Russo and Puleri, 1997) are found to significantly affect the shear capacity of reinforced concrete beams in shear. A combination of all these factors present a major challenge in establishing accurate design equations for safe design of members in shear.

It is reported that that size effect occurs in both short and slender beams with normal strength concrete (Arun and Ramakrishnan, 2014; Korol and Tejchman, 2013). Size effect is represented by a reduction in ultimate shear strength due to increase in beam size (Arun and Ramakrishnan, 2014). However, the experimental information on this subject is limited, especially data on short span and shallow depth beams. The size of a beam is an important factor affecting the shear strength of reinforced concrete beams. This occurs in normal weight concrete beams with and without shear reinforcement (Bazant and Kim, 1984; Bazant and Sun, 1987). The shear strength of reinforced concrete beams without shear reinforcement is found to decrease as the member depth increases, which is called the "size effect" in shear. The main reason for the size effect is attributed to the formation of larger width of diagonal cracks in larger beams which reduces the residual stresses and the ability to transmit shear stresses across crack interface

(Slobe et al., 2012; Matta et al., 2013). This subject is of fundamental and practical relevance in the design of concrete members reinforced with palm kernel shell reinforced beams, especially where PKS beams are of relatively low elastic modulus which stems from the PKS aggregates (Matta et al., 2013; Teo et al., 2006). Previous studies by Jumaat et al. (2009) revealed that reinforced oil palm shell foamed concrete (OPSFC) with shear reinforcement had 50% deflections higher than corresponding NWC beams at ultimate stage.

Knowledge of shear strength capacity of PKS reinforced concrete members without stirrups is of importance in the design process of structural elements. This is because reinforced concrete structural elements such as slabs and foundations do not use shear reinforcement (Rebeiz et al., 2000). Additionally, ACI-318 design procedures also require the determination of the shear-carrying capacity of beams reinforced in bending only before the addition of web reinforcement. Jumaat et al. (2009) have revealed that Oil Palm Shell Foam (OPSF) concrete beams have higher resistance to shear than NWC beams of similar geometrical properties. Acheampong et al. (2015) investigated the influence of stirrups on the behaviour of PKS beams. The results of eight reinforced concrete beams revealed that post-diagonal cracking resistance of PKS concrete beams with shear reinforcement were higher than the corresponding NWC beams. That notwithstanding, the ultimate shear strength of the NWC beams were higher than that of corresponding PKS concrete beams. To fully understand the behaviour of PKS concrete in shear, it is of importance that the influence of beam size and the amount of tension reinforcement on shallow PKS concrete beams be investigated. This is because the type of aggregate influences the aggregate interlock mechanism which in turn affects the shear strength of the concrete beam.

TEST SPECIMENS AND PROCEDURE

Materials

Ordinary Portland cement with a 28-day compressive strength of 42.5 N/mm^2 was used in the study. The fine aggregate used in the study was river sand. The coarse aggregates were crushed PKS with a maximum size of 12.5 mm (for PKS concrete). The shells were flushed with water to remove dust and other impurities. The aggregates were oven dried before determining the physical properties in accordance with BS 812 (1990). Mix proportions of the PKS concrete was in the ratio of 1:1.3:0.6, with a cement content of 550 kg/m^3 . Sika viscocrete, high-range water reducing admixture (1% of weight of cement) was used to improve the workability of the PKSC mix since the water/cement (w/c) was kept low.

Details of beam specimens

Fifteen reinforced PKS concrete beams were cast and tested in the Civil Engineering Concrete Laboratory of KNUST. Considering the

Table 1. Properties of beam specimens and concrete strengths.

Beam ID	Beam size $b \times D$ (mm)	Effective depth d (mm)	Age at testing (days)	Compressive strength, f_c (N/mm ²)	Flexural strength, f_t (N/mm ²)	Tension steel ratio (%)	As provided (mm ²)
P1	120 × 150	119	28	30.3	3.60	1.0	2-R10
P2	120 × 150	119	28	31.1	3.70	1.5	3-R10
P3	120 × 150	114	28	30.5	3.71	2.0	4-R10
P4	120 × 200	168	28	29.8	3.45	1.0	2-R12
P5	120 × 200	168	28	31.7	3.41	1.5	3-R12
P6	120 × 200	163	28	29.5	3.64	2.0	4-R12
P7	120 × 225	193	28	30.3	3.42	1.0	3-R12
P8	120 × 225	193	28	29.4	3.70	1.5	2-R12, 2-R10
P9	120 × 225	187	28	31.7	3.58	2.0	3-R12, 2-R10
P10	120 × 250	218	28	32.3	3.66	1.0	4-R10
P11	120 × 250	216	28	32.3	3.55	1.5	2R16
P12	120 × 250	213	28	30.4	3.74	2.0	3-R12,3R10
P13	120 × 300	263	28	31.7	3.81	1.0	3-R12
P14	120 × 300	263	28	31.1	3.73	1.5	3-R12, 2-R10
P15	120 × 300	259	28	30.3	3.61	2.0	2-R16, 2-R12

overall depth of the beams, five different beam sizes could be identified. The span of test beams was in the ratio of 1:1, 1:1.5, 1:1.7, 1:2.0, 1:2.4 (1000, 1500, 1700, 2000 and 2400 mm). All the beams were 120 mm wide (b) with total depth (D) ranging from 150 to 300 mm (Table 1). The length-to-depth ratio of all beam specimens (L/D) were varied from 6.67 to 8.0. The beam geometries were selected to reflect the common beam dimensions used in real construction. To separate the size effect from other influences, it is worthy to consider members of different sizes but geometrically similar shapes (Bazant, 1984). For example, beams of the same shear span-to-depth ratio. To this end, the loads were positioned so that the shear span-to-depth ratio (a/d) was kept constant at 2.5 to ensure shear modes of failure rather than bending failure of beams. Based on the tension reinforcement (ρ_w), three sets of specimens can be identified, each with five different beam sizes. Deformed mild steel bars of mean yield strength 271.2 N/mm² were used for the tension and shear reinforcement (stirrups). The tension reinforcement had concrete cover of 20 mm to meet at least one-hour fire resistance and a mild condition of exposure, based on clause 3.3.1.2 of BS 8110-1 (1997).

Companion concrete specimens of 150 × 150 × 150 and 100 × 100 × 500 (45 each) were cast to study the compressive and flexural strengths of the beams, respectively. Curing was done using hessian mat spread on the beams in the open atmosphere with regular watering until 28-days.

Beam set up and instrumentation

The beams were simply supported on a stiff steel frame in the Civil Engineering Laboratory of the KNUST, Kumasi. The loads were applied with manually operated hydraulic actuator under crosshead displacement control and were monotonically applied through a stiff steel spreader beam. The spreader beam had sufficient bending capacity to avoid excessive deformation and yielding before failure of the test beam. The observed sides of the beam were white washed to facilitate easy detection and observation of structural cracks as loads were applied.

Beam deflections at mid-span, crack patterns and crack widths were recorded at incremental loading rate of 0.2 kN/s. The

deflections were measured with the aid of a dial gauge with a 0.001 mm accuracy fixed at the soffit of each beam. Crack patterns were outlined by hand with a felt tip pen on the sides of the specimens as they developed, in order to assess the first flexural and shear cracks, and crack widths at tension steel levels. Observation of cracks was performed visually. Selected crack widths were measured using a crack microscope of optical magnification X10 and reading to 0.02 mm. Initiation and propagation of both flexural crack and shear cracks were closely observed and recorded against corresponding applied loads. A schematic sketch of the loading configuration is shown in Figure 1 while a typical loading configuration is shown in Figure 2.

RESULTS AND DISCUSSION

Properties of beam specimens

The results of the compressive and flexural tensile strengths of PKS concrete beams tested at the age of 28 days are presented in Table 1. The average 28-day compressive strength obtained for the beam specimens was about 30.8 N/mm² which was about 3% higher than the target strength of 30 N/mm². The average tensile strength was about 3.62 N/mm² for PKS concrete beam specimens. The results indicate identical mechanical properties of all tested beams. It was noted that failure of the PKS cubes was gradual and along the convex surface, indicating a weak bond between the PKS and the cement matrix. The gradual failure of the cubes is also attributed to the good energy absorbing quality of the PKS aggregates derived from lower aggregate impact and crushing values. Teo et al. (2006) reported that the lower elastic modulus of the PKS concrete results in higher deflection, but beneficially improves the ductility of the concrete. Moreover, the poor adhesion between PKS

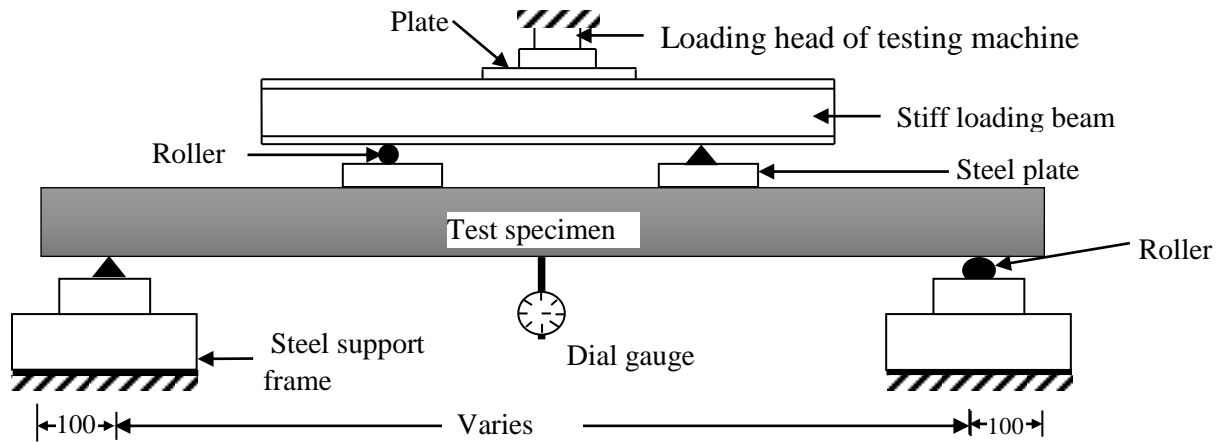


Figure 1. Schematic Diagram of experimental set-up.



Figure 2. Test set up, instrumentation and failure mode.

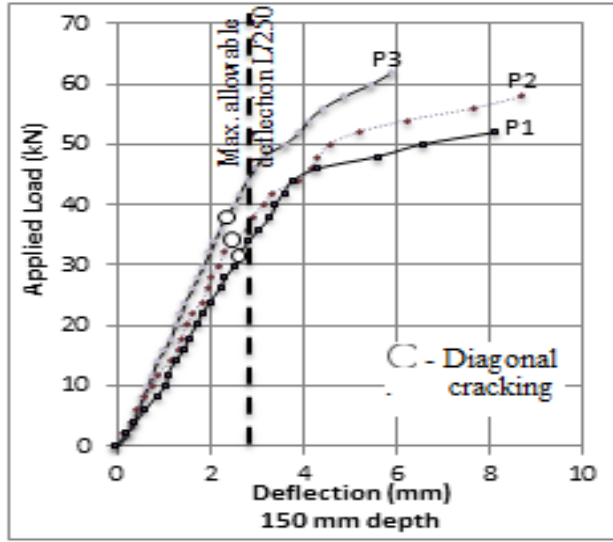
aggregate and cement matrix due to the smooth convex surface of PKS was one of the factors that affected the compressive and flexural strengths of PKS concrete.

Deflection and cracking characteristics of the beams

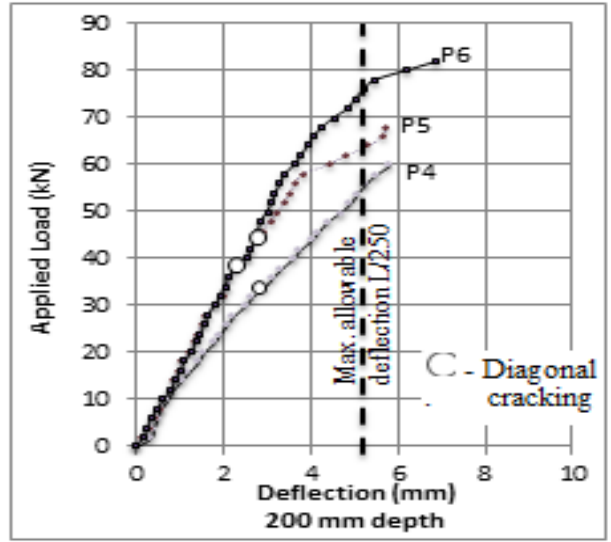
Generally, the load-deflection curves (Figure 3) show that both steel and concrete behaved as a composite material at the initial stages of loading. Thus loads were distributed throughout the specimen until the stress in concrete reached its flexural strength limit, and the first crack appeared in the pure moment zone. The extent of this elastic behaviour depends on the physical properties of the beams (Muyasser et al., 2011). The position and length of the first crack was inconsistent and appeared to be random along the length of the beam. Several other cracks initiated within the shear spans and the pure bending zones with associated increase in applied loads. The ratio of the first flexural crack loads to the failure

loads increased with increase in beam depths having 1.0, 1.5 and 2.0% tension reinforcement (Table 2). First flexural crack loads varied from 16 to 19% of the failure loads for beams with $\rho_w = 1.0\%$. Meanwhile the first flexural crack loads varied from 17 to 29% of the failure load for beams with $\rho_w = 1.5\%$, and varied from 20 to 38% for beams with $\rho_w = 2.0\%$.

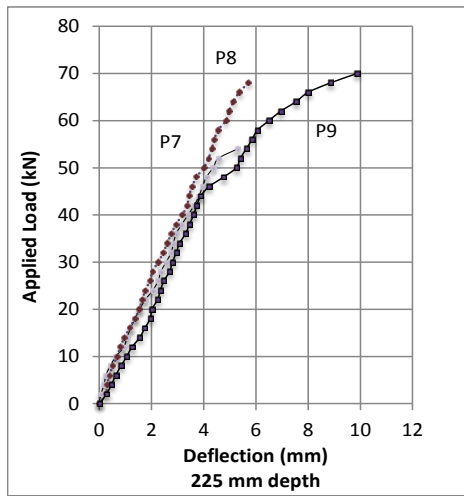
Failure crack patterns of each of the three groups of beams were found to be similar, indicating no significant effect of increasing longitudinal reinforcement ratios. In most cases, diagonal cracks formed independent of previously formed cracks in the shear zone, and gradually turned into inclined cracks under the increasing loads. These cracks spanned diagonally from the lower support to the loading point for all beam specimens. The number and disposition of the cracks were dependent on the amount of longitudinal reinforcement. However, this was in contrast to the increasing size of the beams. It was found that specimens with depths 250 and 300 mm had more cracks and developed wider crack widths at



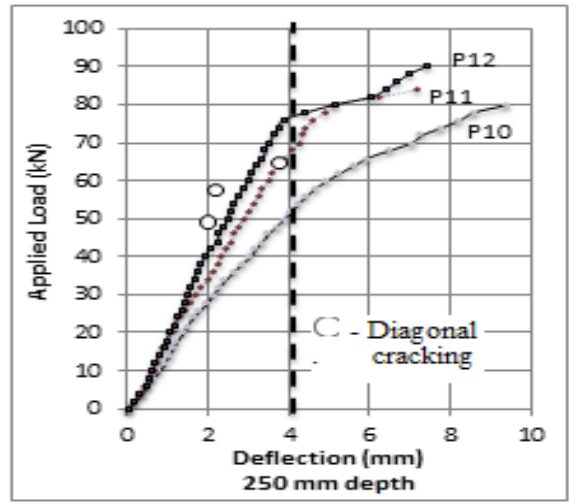
a



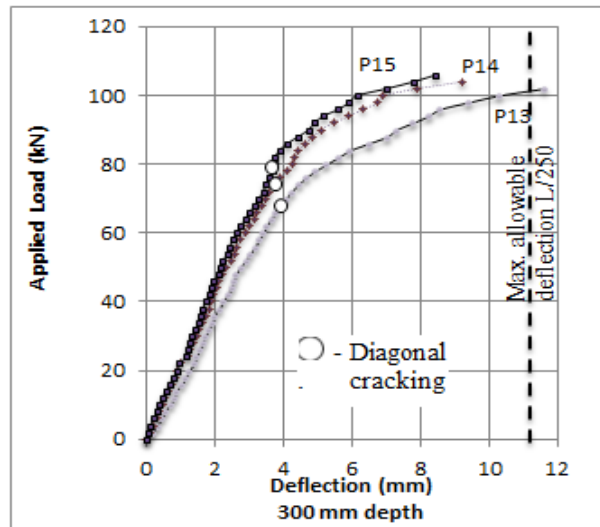
b



c



d



e

Figure 3. (a-e) Load deflection behaviour of PKS beams.

Table 2. Cracking loads and service load deflection.

Beam ID	Total load applied, (P , kN)			Ratio $100P_d/P_u$ (%)	Av. crack spacing, mm	No. of cracks	Max. crack width	Service loads, V_{sl}	Deflection at service loads, mm	Mode of failure
	First flexural crack, P_f	Diagonal crack, P_d	Ultimate failure load, P_u							
P1	10	30	52	58	45	20	0.28	34.7	2.83	FS/DT
P2	12	32	60	53	50	18	0.26	40.0	3.20	FS/DT
P3	14	36	62	58	75	12	0.25	41.3	2.45	FS/DT
P4	12	32	62	52	100	12	0.42	41.3	3.60	FS/DT
P5	14	38	68	56	120	10	0.45	45.3	2.80	FS/DT
P6	18	42	82	51	80	15	0.52	54.7	3.20	FS/DT
P7	12	40	72	56	250	6	0.33	48.0	4.10	FS/DT
P8	14	46	78	59	167	9	0.29	52.0	4.10	FS/DT
P9	18	54	88	61	100	15	0.18	58.7	6.30	FS/DT
P10	14	44	80	55	86	21	0.34	53.3	4.20	FS/DT
P11	18	52	84	62	129	14	0.195	56.0	3.20	FS/DT
P12	30	64	92	70	62	29	0.17	61.3	3.20	FS/DT
P13	18	68	102	67	92	24	0.335	68.0	3.90	FS/DT
P14	30	72	104	69	96	23	0.24	69.0	3.40	FS/DT
P15	40	78	106	74	79	28	0.195	70.7	3.25	FS/DT

Where FS – Flexural-shear; DT - Diagonal tension.

failure depending on the longitudinal reinforcement ratio (Table 2). This could be attributed to increased stresses induced as a result of increased resistance of the concrete section above the neutral axis (Kandekar et al., 2013). In most cases, shear failure of the beams occurred shortly after a dominant diagonal shear crack formed within the shear zone, especially beams of depth 150 and 200 mm. In addition, failure of beams P10 to P15 were very sudden compared to specimens P1 to P9. Since the shear span-to-depth ratio (a/d) was kept constant for all beams, the number of cracks before failure tends to increase with the increasing total depth of the beam. This indicates the effect of increasing size on the cracking behaviour of the beams.

Figure 3 shows that maximum allowable deflections, based on the BS 8110 occurred after diagonal cracking. However, the extent of deflection under the loads depends on the amount of longitudinal reinforcement and the size of the beams. Service load deflections varied from 2.83 to 6.3 depending on the amount of longitudinal reinforcement and the beam size. A closer look at the results in Table 2 reveal that the amount of deflection increases consistently with increasing depth of the beam up to 250 mm. The reduction in deflection for 300 mm deep beams could be attributed to the sudden and brittle modes of failure for increasing beam sizes.

All beams failed as a result of diagonal tension irrespective of the amount of longitudinal steel. This type of failure is very characteristic of beams without shear reinforcement (Oreta, 2004). In addition to the diagonal shear failure, the beams showed bond and anchorage failure at the tension side of the beams, especially in

specimens with $\rho_w = 2.0\%$. In most cases, high stress concentration near the support, which resulted in increased number of cracks at the supports, were associated with the ultimate failure of the beams. The ratio of diagonal cracking to ultimate failure loads varied from 52 to 67% for beam depths varying from 150 to 300 mm at 1% longitudinal reinforcement ratio (Table 2). This ratio varies from 47 to 69% and 51 to 74% for beams with $\rho_w = 1.5$ and $\rho_w = 2.0$, respectively. The average number of cracks varied from 6 to 29. However, the amount of variation was inconsistent with the size of the beam. A closer assessment of the results indicates an increase in the maximum crack widths at failure with increasing beam sizes.

Shear resistance characteristics of the PKSC beams

To analyze and compare the shear strength of beams, the ultimate shear force (V_u) is normalized to account for the difference in compressive strength among the beam specimens. Since the shear strength is proportional to the square root of the compressive strength of concrete (f_c) the normalized shear force (V_n) was determined as follows:

$$V_n = \frac{V_u}{\sqrt{f_c}} \quad (1)$$

The normalized shear stress (V_{ns}) is then calculated as:

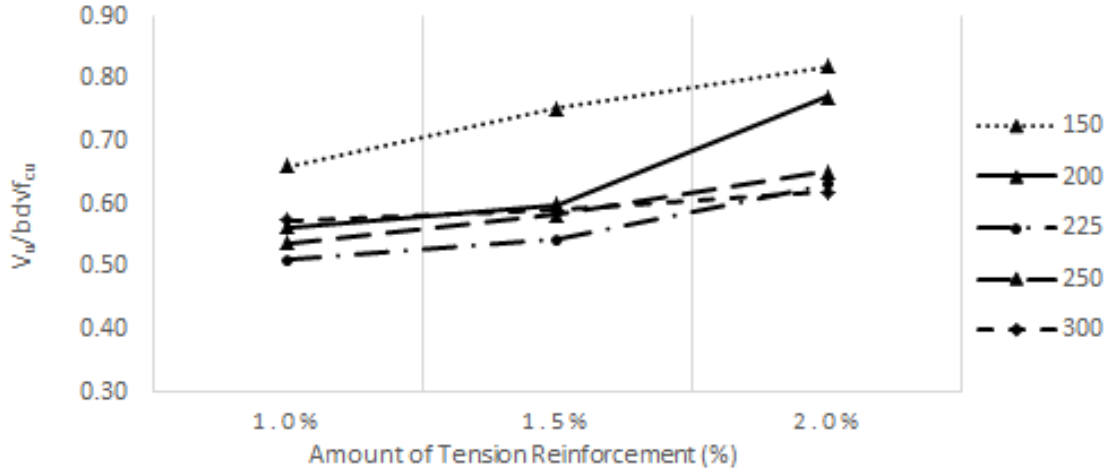


Figure 4. Influence of normalized V_u on varying reinforcement.

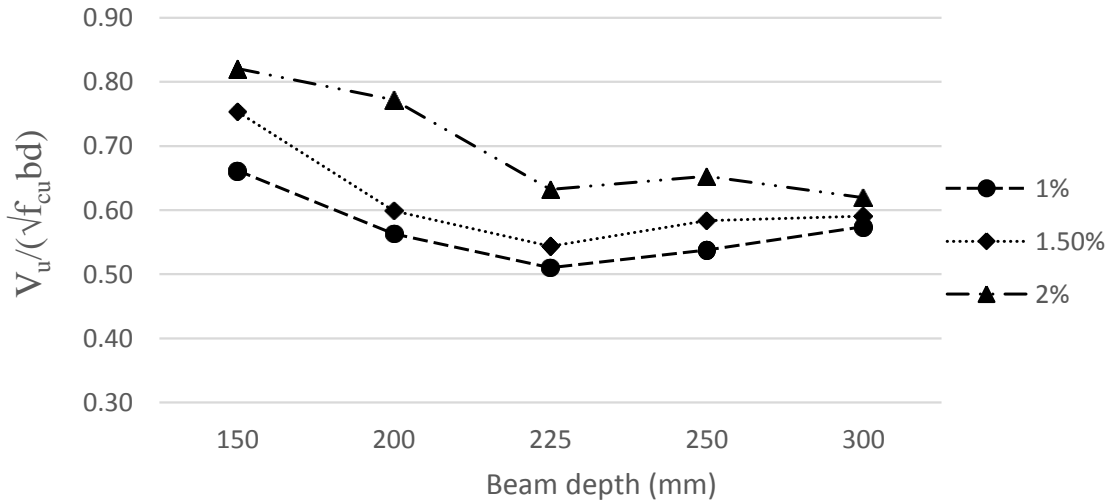


Figure 5. Influence of normalized shear on varying beam depth.

$$V_{ns} = \frac{V_n}{bd} \tag{2}$$

Normalized shear load and stress for all experimental PKSC beams are presented in Figures 4 and 5.

Effect of beam depth on shear strength of PKS reinforced concrete beams

Initial deflections were identical for all dimensions of beams at the various tension steel ratios until the onset of first flexural cracks. Figure 4 shows the variation of $V_u/f_{cu}bd$ as a function of beam depth, d . Generally, the shear strength is found to decrease with increasing depth of the beams. The ultimate normalized shear stress decreased with increase in beam depth as observed by

other researchers for other materials (Matta et al., 2013; Chung-Hao et al., 2011; Hassan et al., 2008). Considering the beams of depth 150 and 300 mm, the amount of loss of strength varied from 16 to 32% depending on the amount of longitudinal reinforcement. At constant reinforcement ratios, the variation in the strength of the beams could be attributed to varying beam depth.

It is observed that as the effective depth increases from 150 to 300 mm, there is a reduction in diagonal cracking shear strength and ultimate shear strength, even though not very significant loss of strength as observed by other researchers for comparatively large beam specimens (Arun and Ramakrishnan, 2014; Hassan et al., 2008). This clearly indicates a size effect in diagonal cracking shear strength and ultimate shear strength of beams at

various tension reinforcement for PKS concrete beams. However, average crack widths and number of cracks were found to be inconsistent with the increasing effective depths of the beams.

Effect of longitudinal reinforcement, ρ_w on deflection and cracking of PKS beams

The amount of longitudinal steel has been shown to greatly affect the shear behaviour of a concrete beam (Figure 5). The important influence of the longitudinal steel ratio, ρ_w on the shear stress at failure is also confirmed as the beams with $\rho_w = 2\%$ were consistently stronger with associated increased failure loads. Generally, deflections decreased while shear stresses increased with increase in longitudinal steel ratios for all test specimens. It is reported that when the longitudinal reinforcement ratios in beams decrease, the shear force carried by the dowel action of longitudinal steel reinforcement decreases (Kong and Evans, 1998). Thus, wider crack widths were observed in beams with lower longitudinal reinforcement ratios.

The effect of the longitudinal steel on the shear strength can also be explained through the aggregate interlock mechanism. In fact, a major component of shear strength in concrete arises from the frictional forces that develop across the diagonal shear cracks by aggregate interlock and the dowel action of the longitudinal reinforcement. This component of shear strength through aggregate interlock is more significant if the cracks are narrow (Ghannoum, 1998). Wider crack widths would reduce the aggregate interlock capacity, and result in lower ultimate failure loads (Kong and Evans, 1998). Subsequently, higher amount of longitudinal reinforcement which reduces the shear crack widths, would allow the concrete to resist more shear (Londhe, 2011). The applied shear stress to initiate diagonal cracking increased with longitudinal reinforcement ratios. The increase in shear stress required is caused by the ability of the increased reinforcement bars to control flexural cracking which disrupts the shear redistribution across the section.

Given the same specimen geometry, the number of cracks, crack widths and their dispositions could be attributed to the amount of longitudinal reinforcement in the tested beam specimens. Crack lengths in specimens with a lower amount of longitudinal reinforcement are found to be longer compared to crack lengths in specimens with higher amount of longitudinal reinforcement ($\rho_w = 1.5\%$ and $\rho_w = 2\%$). That notwithstanding, higher loads were needed to cause the same cracking in the specimens with higher amount of longitudinal reinforcement. Increasing the amount of longitudinal reinforcement resulted in a corresponding increase in diagonal cracking loads for each beam series (Table 2). This may be attributed to the fact that the longitudinal steel has a limited zone of influence in controlling the

formation of diagonal crack widths over increased concrete cross sections. That is, smaller depth specimens will almost entirely be under the influence of the tension steel and have their shear crack widths controlled over most of their heights. Meanwhile the cross-section of larger specimens is only partially influenced by the steel over a limited region. Thus, the larger the specimen, the smaller the zone of influence with respect to the intact compression zone above the neutral axis in a given cross section. Zararis and Papadakis (2001) noted that this compression zone acts as a buffer for preventing any significant contribution of shear slip along the crack interface. Increasing the percentage of longitudinal reinforcement ratio affects the aggregate interlock contribution to shear resistance. Beams with a low percentage of longitudinal reinforcement will have wide, long cracks in contrast to the shorter, narrow cracks found in beams with a high percentage of longitudinal reinforcement (Angelakos, 1999). This increase in shear strength is caused by the ability of the increased tension reinforcement to control flexural cracking which disrupts the flow of shear (Juan, 2011).

A close look at the results in Table 2 reveals that for a given beam series, the number of cracks decreased with increasing amount of longitudinal reinforcement. This is because the increased longitudinal reinforcement ratio controlled the extent of flexural cracking for any given beam series (Elrakib, 2013).

Considering specimens of depths 150 to 200 mm, the average crack width decreased with increasing longitudinal reinforcement while the average crack width increased with increasing amount of longitudinal reinforcement for specimens of depths 225 to 300 mm (Table 2). This may be attributed to the higher influence of the longitudinal reinforcement on smaller depth beams compared to the beams with increased depth. It is also obvious that the greater the number of cracks, the narrower the crack widths (Hassan et al., 2008; Teo et al., 2006; Lim et al., 2007). This is clearly seen from the results in Table 2 where the maximum crack widths decreased with increasing number of cracks for a given beam series at various tension steel levels. As crack widths increase, their ability to transfer shear stresses by aggregate interlock decreases. This may have contributed to the reduced ultimate failure loads in beams with lower reinforcement ratios.

Influence of reserve shear strength index (R) with varying depth

Reserve shear strength index is taken as the ratio of the ultimate shear load to the diagonal cracking load (V_u/V_d) (Arun and Ramakrishnan, 2014). The variation of decreasing reserve shear strength is shown in Figure 6. The reserve shear strength was analyzed from the experimental results in beams of varying sizes and amount of longitudinal reinforcement. The reduction in reserve strength as beam depth increased from 150 to 300 mm

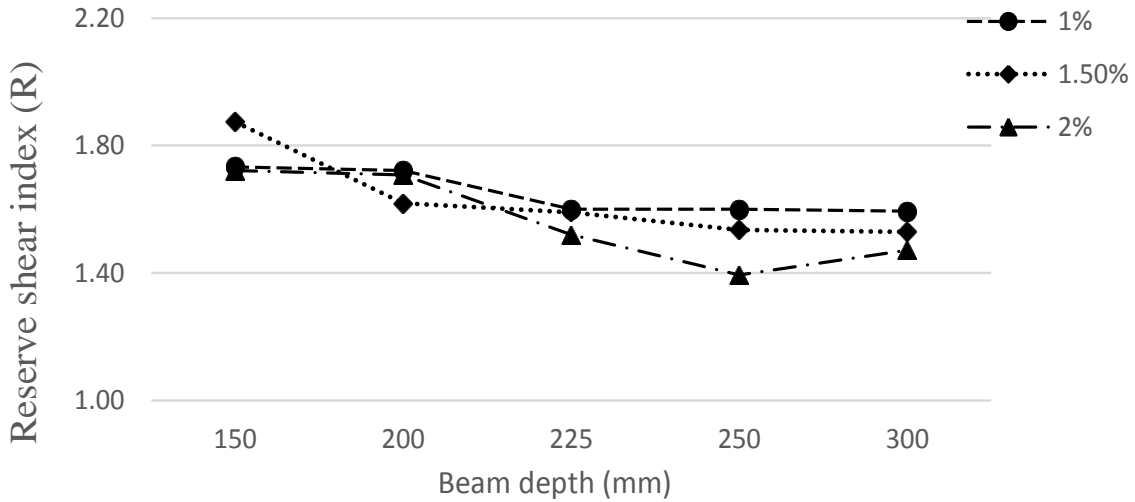


Figure 6. Influence of ρ_w on beam size and reserve strength.

varied from 1.73 to 1.50 for PKS beams with 1% steel reinforcement. The reserve strength varied from 1.88 to 1.44, and 1.72 to 1.36 for PKS beams with 1.5 and 2.0% steel reinforcement, respectively. It seen that increasing the overall depth leads to decrease in load carrying capacity after the diagonal cracking. This results in wider cracks and higher energy released rate at the interface of cracks due to reduction of shear strength (Arun and Ramakrishnan, 2014). A significant loss in reserve strength is found in beams with 2% longitudinal reinforcement ratio and a beam depth of 300 mm, indicating a size effect in the reserve strength of the beams (Figure 6). Comparatively shallow specimens were consistently able to resist higher shear stresses after diagonal cracking than the deeper ones irrespective of the amount of tension steel.

Comparison with code predictions

Concrete contribution to the shear strength of each beam was determined based on the initiation of the first diagonal crack. The concrete contribution was compared with the predictions according to the ACI 318 and BS 8110. The design for shear using the ACI code (ACI 318-08) is based on the shear strength, V_c , of the concrete beam cross-section at diagonal cracking load (Equation 1). A reduction factor of 0.85 is adopted for the design of the PKS beam specimens based on the requirements of the code. This equation considers the effect of longitudinal reinforcement ratio as well as shear to moment ratio ($V_u d/M_u$).

$$V_c = \left[0.16\lambda\sqrt{f'_c} + 17\rho_w \frac{V_u d}{M_u} \right] b_w d \tag{3}$$

where V_u is the factored shear force at section; M_u is the factored moment at section; b_w is the beam width; d is the effective depth of beam cross-section; f'_c is the concrete compressive strength and ρ_w is the longitudinal reinforcement ratio in the beam.

For lightweight aggregate concrete (LWAC) members, BS 8110: Part-2 (1985), adopts the same design parameters as that of normal weight concrete members for concrete grades greater than 25 MPa. In that case, a reduction factor of 0.8 is imposed on the concrete's design stress (V_c) of the normal weight concrete. This factor is also imposed on the maximum limit of shear stress that a section can be subjected to. That is $0.63f_{cu}$ or 4 MPa whichever is lower.

$$V_c = \frac{0.79}{\gamma} \left[\left(\frac{100A_s}{bd} \right)^{1/3} \times \left(\frac{400}{d} \right)^{1/4} \times \left(\frac{f_{cu}}{25} \right)^{1/3} \right] bd \times 0.8 \tag{4}$$

Where A_s is the longitudinal reinforcement; b is the beam width; d is the effective depth; f_{cu} is the compressive strength of concrete

Table 3 presents the results of experimental diagonal cracking loads and code predictions with and without the reduction factors lightweight weight aggregates, based on Equations 1 and 2, for all beam specimens. This comparison is necessary since code predictions are based on the appearance of first diagonal cracks (Acheampong et al., 2015; Juan, 2011).

The BS 8110 and ACI 318 under predicted the diagonal cracking loads (P_d) of the PKS concrete beams irrespective of the beam depth and amount of longitudinal reinforcement. The ratio of experimental to BS8110 predictions with reduction factors range between 1.25 and 1.87 with a mean value of 1.46. Generally, the BS 8110 is found to be more conservative than the ACI. The

Table 3. Experimental results and code predictions.

Beam ID	Diagonal cracking loads, P_d	Theoretical loads with reduction factors				Theoretical loads without reduction factors			
		BS 8110		ACI 318		BS 8110		ACI 318	
		V_{BS8110} (kN)	P_d/V_{BS8110} (%)	V_{ACI318} (kN)	P_d/V_{ACI318} (%)	V_{BS8110} (kN)	P_d/V_{BS8110} (%)	V_{ACI318} (kN)	P_d/V_{ACI318} (%)
P1	30	20.18	1.49	23.48	1.28	25.22	1.19	27.23	1.10
P2	32	23.12	1.38	24.59	1.30	28.90	1.11	28.34	1.13
P3	36	24.97	1.44	24.61	1.46	31.22	1.15	29.44	1.22
P4	32	28.31	1.13	33.22	0.96	32.88	0.97	38.52	0.83
P5	38	30.11	1.26	34.82	1.09	37.64	1.01	40.12	0.95
P6	42	32.73	1.28	35.33	1.19	40.91	1.03	41.71	1.01
P7	40	31.90	1.25	37.84	1.06	39.88	1.00	43.93	0.91
P8	46	33.23	1.38	39.92	1.15	41.54	1.11	46.01	1.00
P9	54	34.66	1.56	40.23	1.34	43.32	1.25	47.61	1.13
P10	44	33.57	1.31	43.94	1.00	41.96	1.05	50.45	0.87
P11	52	36.80	1.41	45.18	1.15	46.00	1.13	51.99	1.00
P12	64	40.28	1.59	46.71	1.37	50.34	1.27	54.18	1.18
P13	68	36.30	1.87	53.50	1.27	45.37	1.50	61.79	1.10
P14	72	41.20	1.75	54.21	1.33	51.51	1.40	62.50	1.15
P15	78	44.29	1.76	55.41	1.41	55.37	1.41	64.57	1.21

degree of conservatism is found to increase with increasing amount of longitudinal reinforcement and beam size, especially for beams with depth ranging from 200 to 300 mm. The ratio of experimental to BS 8110 predictions without reduction factors however, range between 0.97 to 1.50 with an average of 1.17. Considering the results in Table 3, the BS 8110 is found to safely predict the shear strength of PKSC beams with 2% longitudinal reinforcement, irrespective of the size of the beam. The ratio of experimental to ACI 318 predicted values with reduction factors range

between 0.96 to 1.41 with an average of 1.22 depending on the size of beam and the amount of longitudinal reinforcement. Without the reduction factors, the ratio of experimental to ACI 318 predicted values vary from 0.83 to 1.21 with an average of 1.05. This indicates that ACI code may not be safe to design PKS concrete beams without reduction factors which account for the use of lightweight concrete. The ACI equation is found to over predict the shear strength of PKS beams with comparatively deeper sections (300 mm) and higher reinforcement ratios (2%).

Conclusion

The shear resistance of PKS concrete is studied using test results of beams without shear reinforcement. The deflections, cracking loads, crack patterns, crack widths and failure modes are examined in relation to the amount of longitudinal reinforcement and beam geometry. Based on the results, the following conclusions are made:

- (1) The PKS beams showed similar shear resistance characteristics in pre-cracking and post

cracking stages irrespective of the size of the beam. The beams behaved similarly in-terms of crack widths, crack lengths and the overall failure modes. Increasing the depth of beams resulted in a decrease in the ultimate shear strength of the beam specimens.

(2) The results of the study show that the shear strength of PKS concrete increased with the amount of longitudinal reinforcement.

(3) Using the concrete reserve strength, the PKS concrete beams were able to continuously transfer shear loads through other mechanisms until final failure. The reserve strength varied from 88% to 36% depending on the amount of longitudinal reinforcement and beam size.

(4) BS 8110-2 is found to be conservative in predicting the shear strength of PKS beams. The degree of conservatism increases with increasing depth of the beam and the amount of longitudinal reinforcement. The results further show that BS 8110-1 can be used to safely design PKS concrete beams without applying the modification factor of 0.8, especially beam depths of 250 mm and 300 mm and over-reinforced beams.

(5) Although the ACI 318 design for shear is conservative for PKS beams with 2% tension steel irrespective of the beam depth, the degree of conservativeness depends on the depth of the beam. Additionally, the design equation is not conservative for beams with depths ranging from 200 and 300 mm, and 1% tension steel. The ACI equation may not be safe and will over predict the shear strength of PKS beams when the reduction factor of 0.85 is ignored.

Conflict of Interests

The authors have not declared any conflict of interests.

Nomenclature

a_v , shear span; d , effective depth; A_s , area of longitudinal reinforcement; P_d , diagonal cracking load; V , Theoretical failure load; V_u , factored shear force at section; M_u , factored moment at section; b_w , beam width; f'_c or f_{cu} , concrete compressive strength; ρ_w , longitudinal reinforcement ratio in the beam; V_n , normalized shear force; V_{ns} , Normalised shear stress; γ , Partial factor of safety (taken as 1.25); λ , Modification factor reflecting the reduced mechanical properties of LWC.

REFERENCES

- Acheampong A, Adom-Asamoah M, Ayarkwa J, Afrifa RO (2015). Code compliant behaviour of Palm Kernel Shell RC beams in shear. *J. Civ. Eng. Const. Technol.* 6(4):59-69.
- Alengaram UJ, Mahmud H, Jumaat MZ (2010). Comparison of mechanical and bond properties of oil palm kernel shell concrete with normal weight concrete. *Int. J. Phys. Sci.* 5(8):1231-1239.
- Angelakos D (1999). The Influence of Concrete Strength and Longitudinal reinforcement Ratio on the Shear Strength of Large-Size Reinforced Concrete Beams with and without, Transverse Reinforcement, MSc. Thesis, Department of Civil Engineering University of Toronto, USA.
- Arun M, Ramakrishnan S (2014). Size Effect on Shear Behavior of High Strength RC Slender Beams. *Int. J. Res. Eng. Technol.* 03(08):113-118.
- Basri HB, Mannan MA, Zain MFM (1999). Concrete using oil palm shells as aggregate. *Cem. Concr. Res.* 29(4):619-622.
- Bazant PZ, Kim JK (1984). Size Effect in Shear Failure of Longitudinally Reinforced Beams. *ACI Mater. J.* 81:456-467.
- Bazant ZP (1984). Size Effect in Blunt Fracture: Concrete, Rock, Metal. *J. Eng. Mech.* 110(4):518-535.
- Bazant ZP, Sun HH (1987). Size Effect in Diagonal Shear Failure: Influence of Aggregate Size and Stirrups. *ACI Mater. J.* 84(4):259-272.
- Chung-Hao W, Yu-Cheng K, Chung-Ho H, Yen T, Li-Huai C (2011). Flexural behavior and size effect of full scale reinforced lightweight concrete beam. *J. Mar. Sci. Technol.* 19(2):132-140.
- Elrakib TM (2013). Performance evaluation of HSC beams with low flexural reinforcement. *Hous. Build. Natl. Res. Cent. (HBRC) J.* 9:49-59.
- Ghaffar A, Javed A, Rehman H, Kafeel A, Ilyas M (2010). Development of Shear Capacity Equations for Rectangular Reinforced Concrete Beams. *Pak. J. Eng. Appl. Sci.* 6:1-8.
- Ghannoum WM (1998). Size effect on shear strength of reinforced concrete beams. MSc. Thesis, Department of Civil Engineering and Applied Mechanics, McGill University, Canada.
- Hassan AAA, Hossain KMA, Lachemi M (2008). Behavior of full-scale self-consolidated concrete beams in shear. *Cem. Concr. Compos.* 30:588-596.
- Juan KY (2011). Cracking Mode and Shear Strength of Lightweight Concrete Beams. PhD Theses, Department of Civil and Environmental Engineering, National University of Singapore.
- Jumaat MZ, Alengaram UJ, Mahmud H (2009). Shear strength of oil palm shell foamed concrete beams. *Mater. Des.* 30(6):2227-2236.
- Kandekar SB, Dhake PD, Wakchaure MR (2013). Concrete grade variation intension and compression zones of RCC beams. *Int. J. Innov. Res. Sci. Eng. Technol.* 2(8):4067-4072.
- Kong FK, Evans RH (1998). Reinforced and Pre-stressed Concrete. 3rd Edition; Cambridge: E & FN Spon.
- Korol E, Tejchman J (2013). Experimental and Numerical Investigations of Size Effects in Reinforced Concrete Beams with Steel or Basalt Bars, VIII International Conference on Fracture Mechanics of Concrete and Concrete Structures.
- Lim LH (2007). Structural Response of LWC Beams in Flexure, PhD Theses, Department of Civil Engineering, National University of Singapore.
- Loehr RC (1984). Pollution control of agriculture, 2nd ed. Orlando, FL: Academic Press.
- Londhe RS (2011). Shear strength analysis and prediction of reinforced concrete transfer beams in high-rise buildings. *Struct. Eng. Mech.* 37(1):39-59.
- Mannan MA, Ganapathy C (2002). Engineering properties of concrete with oil palm shell as coarse aggregate. *Const. Build. Mater.* 16(1):29-34.
- Mannan MA, Ganapathy C (2003). Concrete from an agricultural waste-oil palm shell (OPS). *Build. Environ.* 39:441-448.
- Matta F, El-Sayed AK, Nanni A, Benmokrane B (2013). Size effect on shear strength of concrete beams reinforced with FRP bars. *ACI Struct. J.* 110(4):617-627.
- Muyasser MJ, Hosam AD, Rao of SM (2011). Flexural Behaviour of Lightweight Concrete Beams. *Eur. J. Sci. Res.* 58(4):582-592.
- Okpala DC (1990). Palm kernel shell as a lightweight aggregate in concrete. *Build. Environ.* 25(4):291-296.
- Oreta AWC (2004). Simulating size effect on shear strength of RC beams without stirrups using neural networks. *Eng. Struct.* 26:681-691.
- Rebeiz KS, Fente J, Frabizzio M (2000). New Shear Strength for Concrete Members Using Statistical and Interpolation Function Techniques. The 8th International Specialty Conference on Probabilistic Mechanics and Structural Reliability. PMC 2000-279.
- Russo G, Puleri G (1997). Stirrup effectiveness in reinforced concrete beams under flexure and shear. *ACI Struct. J.* 94(3):227-238.
- Slobe AT, Hendriks MAN, Rots JG (2012). Sequentially linear analysis

- of shear critical reinforced concrete beams without shear reinforcement. *Finite Elem. Anal. Des.* 50:108-124.
- Teo DCL, Mannan MA, Kurian JV (2006). Flexural Behaviour of Reinforced Lightweight Concrete Beams Made with Oil Palm Shell (OPS). *J. Adv. Concr. Technol.* 4(3):1-10.
- Zararis PD, Papadakis GC (2001). Diagonal Shear Failure and Size Effect in RC Beams Without Web Reinforcement. *J. Struct. Eng.* 127:7(733), 733-742.